Original Article

Asian Pacific Journal of Tropical Biomedicine

journal homepage: www.apjtb.org

doi: 10.4103/2221-1691.326100

Impact Factor: 1.55

Antioxidant, cytotoxic, and anti-venom activity of *Alstonia parvifolia* Merr. Bark

Maria Carmen S. Tan[1]✉, Mary Stephanie S. Carranza[1], Virgilio C. Linis[2], Raymond S. Malabed[1,3], Yves Ira A. Reyes[1], Francisco C. Franco, Jr.[1], Glenn G. Oyong[4]

[1]*Chemistry Department, De La Salle University, 2401 Taft Avenue, Manila 1004, Philippines*

[2]*Biology Department, De La Salle University, 2401 Taft Avenue, Manila 1004, Philippines*

[3]*Department of Chemistry, Graduate School of Science, Osaka University, Osaka 563-0034, Japan*

[4]*Molecular Science Unit Laboratory, Center for Natural Sciences and Environmental Research, De la Salle University, 2401 Taft Avenue, Manila 1004, Philippines*

ABSTRACT

Objective: To evaluate antioxidant, cytotoxic, and anti-venom capacity of crude bark extracts of *Alstonia parvifolia* Merr.

Methods: Gas chromatography-mass spectrometry (GC-MS) and energy dispersive X-ray analyses were accomplished to characterize the chemical constituents of *Alstonia parvifolia*. Biochemical characterization was evaluated using an inhibitory phospholipase A_2 (PLA_2) assay, DPPH, and cytotoxicity assays. Using the constituents listed in the GC-MS analyses, molecular docking was conducted to inspect the binding energies between the chosen compounds and selected PLA_2 isoforms.

Results: GC-MS analyses showed that the *Alstonia parvifolia* crude extract consisted predominantly of acetylmarinobufogenin (14.89%), γ-sitosterol (10.44%), 3-*O*-methyl-*D*-glucose (5.88%), 3,5-dimethoxy-4-hydroxyphenylacetic acid (5.30%), (2α,5α)-17-methoxyaspidofractinin-3-one (AFM) (4.08%), and 2,3,5,6,7,8,9-heptahydro-1-phenyl-5-(*p*-chlorophenylimino)-1H-benzo[e][1,4]thiazepine (HPT) (1.37%). The principal elemental components of *Alstonia parvifolia* were Ca (4.012%) and K (1.496%), as exhibited by energy dispersive X-ray examination. *Alstonia parvifolia* showed significant free radical scavenging ability (IC_{50}: 0.287 mg/mL) and was non-cytotoxic to normal HDFn cells (IC_{50} >100 μg/mL). Moreover, *Alstonia parvifolia* was favorably cytotoxic to MCF-7 (IC_{50}: 4.42 μg/mL), followed by H69PR, HT-29, and THP-1, with IC_{50} values of 4.94, 5.07, and 6.27 μg/mL, respectively. *Alstonia parvifolia* also displayed notable inhibition against PLA_2 activity of *Naja philippinensis* Taylor venom with IC_{50} of (15.2 ± 1.8) μg/mL. Docking and cluster analyses projected negative binding energies from AFM (−6.36 to −9.68 kcal/mol), HPT (−7.38 to −9.77 kcal/mol), and acetylmarinobufogenin (−7.22 to −9.59 kcal/mol). These calculations were for the particular interactions of *Alstonia parvifolia* constituents to PLA_2 homologues where the utmost affinity was detected in HPT owing to the dipole interactions with amino acid residues.

Conclusions: The bark extract of *Alstonia parvifolia* shows great potential as an anti-venom agent due to its low cytotoxic profile, remarkable PLA_2 inhibition, and docking binding energies between its bioactive constituents and PLA_2 homologues.

KEYWORDS: *Alstonia parvifolia* Merr.; *Naja philippinensis* Taylor; Gas chromatography-electron ionization-mass spectrometry; Secretory phospholipase A_2; Cytotoxicity assay; Anti-venom

1. Introduction

In communities with underdeveloped health care systems, concoctions from recognized herbal sources such as the bark from *Alstonia* sp. have been employed as traditional medicine. *Alstonia parvifolia* (*A. parvifolia*) Merr. is a small tree (maximum height of 8 m) with glabrous branches and leaves in whorls of four[1].

✉To whom correspondence may be addressed. E-mail: maria.carmen.tan@dlsu.edu.ph

How to cite this article: Tan MCS, Carranza MSS, Linis VC, Malabed RS, Reyes YIA, Franco Jr. FC, et al. Antioxidant, cytotoxic, and anti-venom activity of *Alstonia parvifolia* Merr. Bark. Asian Pac J Trop Biomed 2021; 11(10): 460-468.

Article history: Received 5 January 2021; Revision 8 April 2021; Accepted 25 June 2021; Available online 30 September 2021

This species is endemic to the Philippines and is found in the few localities of the island of Luzon, in Negros island, and on Mount Kinabalu in the island of Borneo. *A. parvifolia* occurs in scattered populations consisting of only a few trees of secondary growth in areas such as logged-over forests, rocky forested slopes, and along exposed ridges[2]. Despite its close affinity to two medicinally important plants, *Alstonia scholaris* (L.) R.Br. and *Alstonia macrophylla* Wall. ex, *A. parvifolia* has no reported or identified traditional medicinal use[3,4].

From a 2019 report from the World Health Organization (WHO), nearly 5.4 million people are bitten by snakes annually. Statistics have shown that this corresponds to 2.7 million envenomed individuals, 400000 sufferers sustaining physical impairments, and 138000 casualties[5]. In 2013, WHO reinstated snake envenomation to the list of neglected tropical diseases due to the increasing number of deaths per year. The routine use of anti-venom serum or immunoglobulin (AVS) remains to be the first and foremost medical protocol for the disease; however, its use persists to be a critical health hazard for victims internationally[6]. Conventionally, snake anti-venoms are produced by developing hyperimmune serum in animals (such as horses) as an agent against snake venoms. The extracted serum is then purified to isolate whole immunoglobulin G fractions. These isolates are then further fractionated and purified to attenuate unfavorable side effects and augment efficacy in envenomed patients[7]. Granting that recent technology has led to the advancement of far superior commercially obtainable AVSs, undeniable scientific obstacles have yet to be overcome, such as lack of funding and government support in raising animal models, increasing the reliability of these hosts, and the accessibility/feasibility of such methods to produce the AVS. As a consequence, anti-venom research has trailed behind other researches and has been overlooked despite its life-long impact on victims and the alarming increase in deaths per year.

Particularly in the Philippines, the toxic venom of the cobra species *Naja philippinensis* (*N. philippinensis*) (Philippine Cobra) has beleaguered rice farmers from Bicol and Nueva Ecija. In these regions, the number of recorded cases of snakebites is high and is a great cause for alarm. Folk medicine has been a reliable alternative for locals in rural areas of the Philippines to treat snake envenomation. Previous studies have shown that the bark and leaves of medicinal *Alstonia* species can hinder the effects of viper envenomation in animal experiments[8], which makes this plant more interesting to study as to its possible use as an anti-venom agent.

In this research endeavor, we ascertained the antioxidant capacity, cytotoxic activity (HT-29, H69PR, MCF-7, THP-1 immortalized cell lines and normal HDFn primary culture cells), and anti-venom activity of crude *A. parvifolia* extracts. Chemical characterization was achieved using a gas chromatograph in tandem with a mass spectrometer and an energy dispersive X-ray (EDX) spectrometer.

2. Materials and methods

2.1. Plant material

The bark of *A. parvifolia* Merr. was gathered from Mariveles, Bataan, Philippines and was authenticated by Virgilio Linis, a botanist from De La Salle University. The aforementioned plant was submitted to the De La Salle University Herbarium with a voucher specimen number: 5804-17.

2.2. GC–EI–MS analysis

A. parvifolia bark (4.2 g) was pulverized and solvent-extracted with 50:50 methanol/dimethylsulfoxide (MeOH/DMSO, mass spectrometry grade) as stipulated by a previously described technique[9]. The subsequent mixture was filtered using filter paper (Whatman 91) and then dried under nitrogen gas for 1 h. The crude extract afforded approximately 0.7 g and was reconstituted in 1 mL MeOH. The resultant sample was then filtered through a syringe with a 0.45 μm nylon membrane before commencing investigations.

A. parvifolia samples were studied employing an Agilent gas chromatograph-mass spectrometer (GC-MS) 7890B, an HP-5ms (5% phenyl methylsiloxane) Ultra Inert column (30 m × 250 mm × 0.25 mm), and ultra-pure helium gas as the mobile phase for the examination of vaporizable components. The constraints of helium gas were automated to the following parameters: flow rate of helium gas was at 1 mL/min, pressure fixed at 8.2 psi, with a mean velocity of 36.62 cm/s, and holdup time of 1.37 min. The splitless inlet was conserved at 250 ℃ at 8.2 psi, with an overall flow speed of 24 mL/min, and a septum purge flow speed of 3 mL/min. The injector temperature was retained at 250 ℃. The temperature gradient program began at 70 ℃ and the preset stepwise escalation of the temperature to 2 ℃/min was achieved until the maximum of 135 ℃ was reached and this temperature was maintained for an additional 10 min. After the hold period, an additional temperature increment of 4 ℃/min was implemented to attain the required temperature of 220 ℃ after which this temperature was retained for 10 min. The temperature was then augmented to 270 ℃ at a rate of 3.5 ℃/min and this fixed temperature was maintained for 37 min.

Compound identification was accomplished by means of the NIST library, 2.0 and percent peak area average was managed from the subsequent total ion chromatograms. The consequent data was established by the assessment of the analytes according to their elution succession on a non-polar stationary phase. The retention indices were computed for the entirety of the compounds using a homologous series of *n*-alkanes. The experiments were undertaken in three replicates.

2.3. EDX analysis

Dried samples of *A. parvifolia* bark were positioned in a 10 mm

Mylar cup for elemental exploration using an EDX-7000. The experiments were achieved with the collimator set at 10 mm and the atmosphere was in vacuo.

2.4. Free radical scavenging assay

The free radical scavenging capability of *A. parvifolia* was evaluated by an adjusted DPPH assay methodology[10]. A total of 0.5 mg of ground bark biomass was mixed to 1 mL of 7.0 mL MeOH, 2.95 mL H_2O and 0.05 mL HCl. The sample was incubated in the aforementioned solution for 3 h, and filtered (Whatman 91), and the eluents were then concentrated by drying under nitrogen gas for 2 h to yield 50 mg of crude extract.

Afterwards, 3.94 mg of 1, 1-diphenyl-2-picrylhydrazyl (DPPH) in 50 mL of methanol was made to formulate a 0.2 mM DPPH solution. An original starting concentration of 4 mg/mL of *A. parvifolia* was made. The negative control consisted of 1 mL of DPPH solution with 1 mL of methanol. Reaction mixtures consisting of 1 mL *A. parvifolia* extracts (17.5 to 0.27 mg/mL) and 1 mL of 0.2 mM DPPH solution were incubated at ambient temperature for 30 min and the absorbance of each trial was monitored at 515 nm (UV-Vis Hitachi spectrophotometer 2900). The IC_{50} value was deducted through linear interpolation from the regression equation. Inhibition of the DPPH free radicals in solution was established by the following equation:

DPPH scavenging effect (%)=$[(A_0-A_1)/A_0] \times 100$

Where A_0 is the absorbance of negative control and A_1 is the absorbance of sample.

2.5. Cell viability assay

The corresponding extraction procedure used for the GC-MS trials was also followed for the cytotoxicity experiments on the subsequent human cell lines (ATCC, Manassas, Virginia, U.S.A.): breast cancer (MCF-7), colon cancer (HT-29), small cell lung carcinoma (H69PR), human acute monocytic leukemia (THP-1); and a primary culture of normal human dermal fibroblast, neonatal (HDFn) (ThermoFisher Scientific, Gibco®, USA). The immortalized cells were generously provided by the Cell and Tissue Culture Laboratory, Molecular Science Unit, Center for Natural Sciences and Environmental Research, De La Salle University. Culture and maintenance were performed in complete Dulbecco's Modified Eagle Medium with 10% fetal bovine serum and 1× anti-biotic, anti-mycotic (Thermo Fisher, Invitrogen, USA) and were incubated at 37 ℃ with 5% CO_2 and 95% humidity. The parameters concerning the *in vitro* assays were reported in our previously published work and strictly followed in this work[11]. Zeocin, an intercalating agent, was used as the positive control. Optical density (OD) was measured at 570 nm and was used to ascertain the percent cell viability following the equation:

$$\text{Cell viability } \% = \frac{(OD_{\text{Treated sample}} - OD_{\text{Blank}})}{(OD_{\text{Negative control}} - OD_{\text{Blank}})} \times 100$$

2.6. In vitro inhibitory secretory phospholipase A_2 ($sPLA_2$) activity

The anti-venom potential of *A. parvifolia* on $sPLA_2$ of *N. philippinensis* venom was determined through a $sPLA_2$ targeted commercially available kit (Secretory Phospholipase A_2 Assay Kit Cat. No. ab133089) purchased from Abcam® (Cambridge, United Kingdom). The reagents of the assay kit were formulated as indicated by the information sheet accompanying the kit. The protocol that was used for the experiments and resulting calculations were the same as those reported in our earlier published work[11].

2.7. Molecular docking study

Autodock Vina was used for the initial screening of several protein candidates which are known to be present in the *N. philippinensis* venom such as the following: phospholipases, neurotoxins, and cardiotoxins[12,13]. Autodock 4.0 was used for the scrutiny of the top protein target candidates from the screening with PDB IDs: 1LN8, 1S6B, 1PSH, and 1A3F. Lamarkian Genetic Search algorithm was used for the docking of (2α,5α)-17-methoxyaspidofractinin-3-one (AFM), 2,3,5,6,7,8,9-heptahydro-1-phenyl-5-(*p*-chlorophenylimino) (1H) benzo[e][1,4]thiazepine (HPT), and acetylmarinobufogenin (AMB) into the protein candidates. A grid box encompassing the entire protein structure for each target was established (blind docking). Independent 200 GA iterations with a population size of 150, 2 500 000 assessments, and 27 000 maximum generations were executed for each target protein, respectively. The 200 docking conformations of the ligands, generated for each target, were scored based on the calculated binding energy and were clustered corresponding to the root mean squared deviation.

2.8. Statistical analysis

Statistical assessments were performed using the software GraphPad Prism 7.01 (GraphPad Software, San Diego, CA, USA). Acquired data values were evaluated by one-way analysis of variance (ANOVA) as well as Tukey's post-test for multiple comparisons among particular test sets.

3. Results

3.1. GC–EI–MS characterization of A. parvifolia extracts

Six constituents were identified in *A. parvifolia* extracts. The

identified components of the volatile compounds of the crude extract were verified by retention index and structural class *via* the NIST library generated from the resultant peaks in the chromatogram (Supplementary Figure 1). The *A. parvifolia* crude extracts were comprised of the detected constituents: one compound with diverse functional groups, HPT (1.37%); a steroid, AMB (14.89%); a triterpenoid, γ-sitosterol (10.44%); an alkaloid, AFM (4.08%); a carbohydrate, 3-*O*-methyl-*D*-glucose (5.88%); and a phenolic acid, 3,5-dimethoxy-4-hydroxyphenylacetic acid (5.30%). The compounds are itemized in Table 1 according to their elution succession through an HP-5ms column.

3.2. EDX analysis of A. parvifolia extracts

The elemental components obtained exhibited the following percentages: (<ppm) of Ca (4.012%), K (1.496%), Cl (0.934%), S (0.898%), Si (0.0.084%), Fe (0.022%), Zn (0.0013%), with glucose, $C_6H_{10}O_5$ consisting of 92.287%. The X-ray energy spectrum is presented in Supplementary Figure 2.

3.3. Free radical scavenging activity of A. parvifolia extracts

A. parvifolia extracts demonstrated significant antioxidant activity in DPPH assay with an IC_{50} value of 0.287 mg/mL (Figure 1).

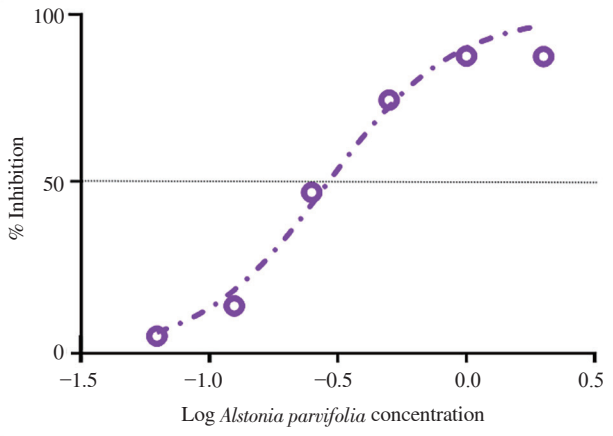

Figure 1. Free radical scavenging activity of MeOH/DMSO fractions of *Alstonia parvifolia* bark.

3.4. Cytotoxicity of A. parvifolia extracts

The anti-proliferative action of the crude extract of *A. parvifolia* was explored on MCF-7, H69PR, HT-29, THP-1, and HDFn immortalized cell lines. An IC_{50} value exceeding 100 μg/mL was obtained, indicating *A. parvifolia* extracts were non-cytotoxic to HDFn cells. Cytotoxic properties of *A. parvifolia* and zeocin on the viability of the individual cell lines are demonstrated in Figure 2. Dose-response curves of *A. parvifolia* on MCF-7, H69PR, HT-29, THP-1, and HDFn are shown in Supplementary Figure 3. Similar activity with respect to IC_{50} was observed between MCF-7 (IC_{50}: 4.42 μg/mL), H69PR (IC_{50}: 4.94 μg/mL), and HT-29 (IC_{50}: 5.07 μg/mL). Moreover, there were no significant differences in IC_{50} of H69PR, THP-1 (IC_{50}: 6.27 μg/mL), and HT-29 cell lines. The normal cells, HDFn, were not disrupted by *A. parvifolia* (IC_{50}>100 μg/mL). Zeocin gave IC_{50} values of 3.37 μg/mL (MCF-7), 3.83 μg/mL (H69PR), 3.78 μg/mL (HT-29), 3.59 μg/mL (THP-1), and 4.08 μg/mL (HDFn). Multiple comparisons of *A. parvifolia* and zeocin displayed that these two inhibitors showed comparable activity on both MCF-7 and H69PR.

3.5. Inhibitory $sPLA_2$ activity of A. parvifolia

The *A. parvifolia* bark showed remarkable inhibition against the phospholipase activity as displayed by the IC_{50} concentration of (15.2 ± 1.8) μg/mL (Figure 3).

3.6. Molecular docking study

For this study, the best candidates were preliminarily screened on several PLA_2 homologues. Four structures: 1LN8, 1S6B, 1PSH, and 1A3F were chosen for further docking analysis. The chosen crystal structures of PLA_2 proteins are found in the venom of *Napa* species. Three compounds, AFM, HPT, and AMB, were chosen to depict the various binding energies when docked to protein isoforms of PLA_2 (Supplementary Figures 4-6 and Supplementary Tables 1-3). Supplementary Tables 1-3 present the binding energy values generated from the docking simulations and Supplementary Figure 7 illustrates the 2D and 3D chemical structures of AFM, HPT, and AMB. Negative binding energies were observed for the binding of AFM to PLA_2 proteins, especially for the *Naja naja* 1PSH homologue at −9.68 kcal/mol. This was followed by the 1S6B, 1LN8, and 1A3F homologues of the phospholipase enzyme with −7.92 kcal/mol, −7.89 kcal/mol, and −6.60 kcal/mol, respectively.

Table 1. Constituents of *Alstonia parvifolia* extracts.

Compound	RT (min)	RI[a]	% Peak area	Functionality
3-*O*-Methyl-*D*-glucose	47.29	1 731	5.88	Carbohydrate
3,5-Dimethoxy-4-hydroxyphenylacetic acid	51.07	1 802	5.30	Phenolic acid
(2α,5α)-17-methoxyaspidofractinin-3-one	87.24	2 866	4.08	Alkaloid
Acetylmarinobufogenin	88.36	2 908	14.89	Steroid
2,3,5,6,7,8,9-Heptahydro-1-phenyl-5-(*p*-chlorophenylimino)-1H-benzo[e][1,4]thiazepine	91.39	2 946	1.37	Diverse functional group
γ-Sitosterol	96.48	3 026	10.44	Triterpenoid

[a]Retention index (HP-5 ms column); RT: retention time.

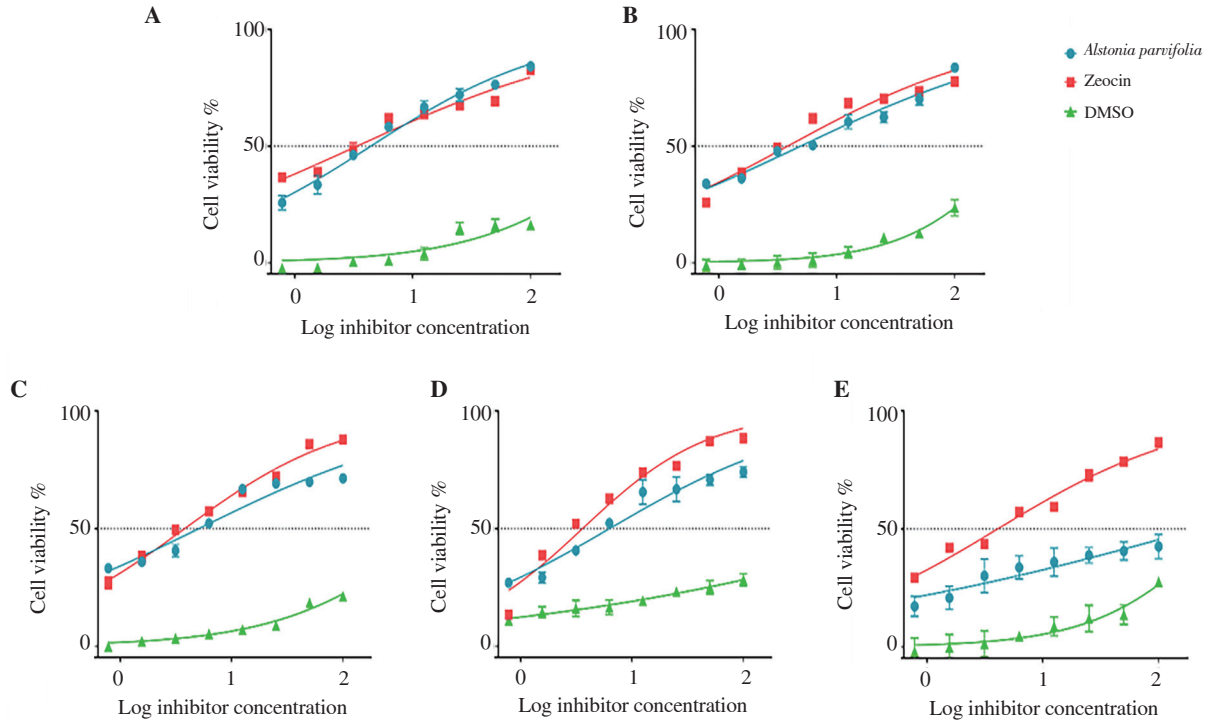

Figure 2. Dose-response curves showing the effect of *Alstonia parvifolia*, zeocin, and dimethyl sulfoxide (DMSO) on the cell viability of (A) MCF-7, (B) H69PR, (C) HT-29, (D) THP-1, and (E) HDFn. Each plot displays the effect of *Alstonia parvifolia* and controls against each cell line. Data are shown as mean ± SEM. GraphPad Prism 7.01 was used to perform extra sum-of-squares *F*-test to (A) evaluate the significance of the best-fit-parameter (half maximal inhibitory concentration) among different treatments, and to (B) determine the differences among the dose-response curve fits. MCF-7 F(Dfn, DFd) = (A) F (2, 21) = 28.58, $P < 0.001$ and (B) F (2, 48) = 5325, $P < 0.001$; H69PR (A) F (2, 21) = 29.12, $P < 0.001$ and (B) F (2, 48) = 5707, $P < 0.001$; HT-29 (A) F (2, 21) = 24.34, $P < 0.001$ and (B) F (2, 46) = 9518, $P < 0.001$; THP-1 (A) F (2, 21) = 21.40, $P < 0.001$ and (B) F (2, 46) = 3697, $P < 0.001$; HDFn (A) F (2, 21) = 26.79, $P < 0.001$ and (B) F (2, 48) = 969.4, $P < 0.001$.

HPT conformations demonstrated highly negative binding energies. The results of HPT are arranged as follows in decreasing binding energies: 1S6B (−9.77 kcal/mol), 1PSH (−9.66 kcal/mol), 1A3F (−9.39 kcal/mol), and 1LN8 (−8.74 kcal/mol). Finally, AMB conformations to $sPLA_2$ homologues also exhibited varying negative binding energies and are as follows: 1PSH (−9.59 kcal/mol), 1S6B (−9.41 kcal/mol), 1LN8 (−8.43 kcal/mol) and 1A3F (−7.75 kcal/mol). It is important to note that for multimeric structures, the docking simulation was only done to a single monomer to lower computational resources.

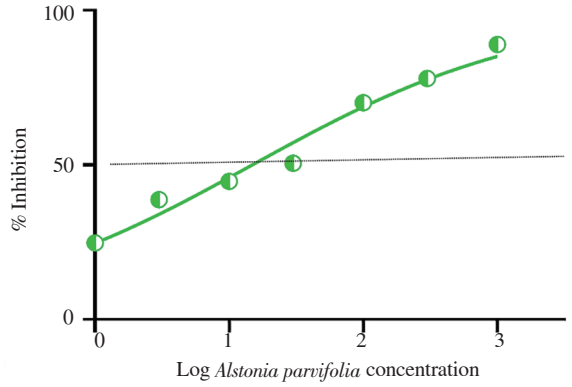

Figure 3. The inhibitory effect of *Alstonia parvifolia* against secretory phospholipase A_2 activity.

4. Discussion

Six bioactive compounds were present in the crude MeOH/DMSO bark extract of *A. parvifolia*. AMB is a steroid lactone derivative that belongs to a class of compounds called bufogenin. Although previous studies are limited to the biochemical mechanism of AMB, steroids of this class are known to have anti-cancer, anti-tumor, and anti-proliferative properties[14–16]. Furthermore, the benzothiazepine ring found in the structure of HPT was found to contribute to its selectivity for vascular calcium channels which suggests its possible role in slowing the absorption of scorpion toxins[17].

Alkaloids have demonstrated their suppressive activity towards the basic PLA_2 enzyme and hyaluronidase enzyme. This compound class is widely distributed in the plant matrices studied and has been linked to local hemorrhages which assist in the spread of the toxin. In other studies, alkaloids have exhibited their ability to neutralize the lethality and myotoxicity induced by pit viper venom[18]. More specifically indole alkaloids, like that of AFM, were isolated from the latex of *Tabernaemontana catharinensis* (also from the *Alstonia* plant family Apocynaceae) and were found to be potential candidates for screening against snake phospholipases and metalloproteases[19]. Among the various chemical groups found in the *A. parvifolia* extract were phytosterols. The compound found in the extract, γ-sitosterol,

has been reported to take part in the mechanism of venom neutralization through its anti-hemorrhagic, anti-neurotoxic, and anti-myotoxic properties according to an *in vivo* study[20,21]. Compounds identified in the MeOH/DMSO *A. parvifolia* extract allude to several possible contributing factors that make *Alstonia* species a potential anti-venom therapeutic alternative. These bioactive constituents may take part in either one or several mechanisms, principally in the inhibition of enzyme activity and protein precipitation.

Raised concentrations of potassium (K) and calcium (Ca) indicated that the plant accrued an elevated quantity of mineral nutrient absorption from the soil. There have been reports on improved lipid blood chemistry, glucose metabolism, and blood pressure due to calcium ingestion in healthy elderly women[22,23]. Assimilation of potassium-rich foods has been found to initiate regulation of blood pressure and cardiovascular anomalies, alleviate bone and renal disease, and prevent strokes[24].

A. parvifolia extracts were found to be effective free radical scavengers given that the IC_{50} value was low at 0.287 mg/mL, which was comparable to other reported values of other leading medicinal plants (IC_{50}: 0.79 mg/mL)[25]. The antioxidant capacity of *A. parvifolia* can be related to its high alkaloid content. Alkaloids, due to the presence of the nitrogen atom in the heterocyclic ring, have been known to successfully diminish reactive oxygen species[26]. Reactive oxygen species have been related to a variety of degenerative illnesses specifically cardiovascular disease and malignancies due to genetic damage[27]. Compounds that act as eliminators of free radicals have also been found to assist in the inhibition of PLA_2 activity[28].

The unpaired *t*-test difference in mean value scores of *A. parvifolia* and zeocin was insignificant, demonstrating the comparable antiproliferative action of both *A. parvifolia* and zeocin on aberrant cell lines. The result also showed that the cytotoxic activity against H69PR and THP-1 cells exhibited no significant differences between the two inhibitors ($P>0.05$).

Assessment of the effectiveness of *A. parvifolia* on the four immortalized cancer cell lines revealed that the integrity of MCF-7, H69PR, HT-29, and THP-1 consistently decreased in all the trials and the action of cytotoxicity was analogous to the positive control zeocin. All the cancer cell lines were highly responsive to *A. parvifolia*. *A. parvifolia* were non-cytotoxic to HDFn with an IC_{50} value greater than 100 μg/mL, whereas zeocin treated normal cells reached their half-maximal inhibitory concentrations at less than 5.00 μg/mL.

The anti-proliferative capacity of the extracts was linked to the high concentration of the alkaloids AFM and AMB. Though no activity has been reported with AFM, AMB was found to be cytotoxic to drug-resistant CEM/ADR5000 cells [IC_{50}: (1 090.0 ± 33.0) nM]. This was reported with a subdued 1.2 degree of resistance relative to the cross-resistance of established anticancer drugs such as doxorubicin (<1 000 fold), vincristine (<400-fold), paclitaxel (<200-fold) and others[29].

Epidemiological research has proposed that phytosterols such as sitosterol, a constituent of *A. parvifolia*, could prevent the onset of certain cancers. Hormone insensitive cancer cells MDA-MB-231 treated with 16 μM β-sitosterol for 3 d exhibited a 70% reduction in cell development. This phytosterol manifested the downregulation of cholesterol synthesis from mevalonate and the upregulation of the MAPK pathway correlating to the inhibition of MDA-MB-231 cell growth[30].

The amplification of snake venom toxicity is triggered through several signaling pathways which involve a range of proteins and molecules. This includes the snake venom phospholipases (sPLA), which leads to an increase in arachidonic acid, intracellular Ca^{2+}, and nicotinic receptor deactivation when activated[31]. The $sPLA_2$ activity of 100 μg/mL *N. philippinensis* venom was examined in the presence of the potential inhibitor *A. parvifolia*. Seven concentrations of plant extracts ranging from 1 μg/mL to 1 000 μg/mL were tested against 100 μg/mL *N. philippinensis* venom. The $sPLA_2$ activities in the presence of inhibitors were determined and compared with that of *N. philippinensis* venom in the absence of inhibitors [(0.084 ± 0.002) μmol/min/mL]. The *A. parvifolia* bark demonstrated significant inhibition of phospholipase activity as displayed by the low concentration of the IC_{50} [(15.2 ± 1.8) μg/mL].

1LN8 and 1S6B are different isoforms of PLA_2 from *Naja sagittifera*. The differences between the two isoforms are in their structure and organization. 1LN8 was crystallized as a monomer while 1S6B was crystallized as a dimer where the bound calcium ions (Ca^{2+}) were crowded by interactions with amino acid residues and free phosphate ions[32]. 1PSH and 1A3F are crystal structures of PLA_2 from *Naja naja*. 1PSH was crystallized with the bound Ca^{2+} intact, whereas 1A3F was crystallized independently under Ca^{2+}-free conditions[33,34].

The highly negative binding energies were predicted for the binding of AFM to PLA_2 proteins. The negative binding energies were due to the various non-bonding interactions of AFM with the active site residues of the four proteins. In this study's modeling, default settings were used for Autodock and the simulations in the ligand-amino acid interactions. The best binding of AFM was observed in AFM-1PSH with a top pose that generated binding energy of −9.68 kcal/mol due to the eleven residues interacting with AFM. One specific interaction was with an H-bond between O_{23} of AFM and His47. Overall, the binding energies of AFM to the other proteins suggested that it is highly likely for AFM to inhibit PLA_2 proteins. Thus, the observed experimental anti-venom properties of the compound could be linked to the inhibition of PLA_2 in *N. philippinensis* venom. It is known that PLA_2 is a critical compound for snake venoms as they facilitate the lysis of cell membranes of prey cells[35]. Therefore, the inhibition of PLA_2 proteins is a possible mechanism in the decreased venomous activity of the snake toxin in the presence of AFM.

It was observed that, in addition to the interactions between amino acids, proteins that contain bound Ca^{2+} (1LN8 and 1PSH) had higher binding energy compared to proteins without the presence of bound Ca^{2+} (1S6B and 1A3F) which is available to interact with the ligand. To further investigate the importance of Ca^{2+} and other residues in binding AFM, the "best pose" of AFM was examined for each receptor and is shown in Supplementary Figure 4. Regarding 1PSH, the best pose belonged to the most populated cluster which demonstrated that the binding of AFM to this protein would likely occur in the vicinity of the top pose. However, as we show in Supplementary Table 1, varying clusters of poses exhibited comparable binding energy values. It was also observed that certain clusters with less favorable binding energy values were more populated such as cluster 3 for 1LN8 and 1A3F. This implies that the proposed structures shown in Supplementary Figure 4 may not necessarily be the optimal binding position that AFM would assume when binding to these receptors *in vivo* and there is no way to confirm that using purely docking analysis. Results have shown that when Ca^{2+} (green spheres in 1LN8 and 1PSH) was present in the protein structures, AFM had direct contact with Ca^{2+} and gave the most favorable binding energy with the ligand. This indicated that the presence of bound Ca^{2+} helped in the binding of AFM to PLA_2 proteins. This was especially true for 1PSH where the highest binding energy observed was due to the affinity of the Ca^{2+} ion to the electron-rich region (red regions) of the ligand. In contrast, the binding of AFM to 1A3F was limited to the outer surface resulting in the lowest binding energy docking results. Among the four PLA structures, AFM generated only −6.60 kcal/mol for the most optimal pose. The computational analyses provided a molecular explanation for the observed promising *A. parvifolia* activity in the $sPLA_2$ inhibition experiments performed.

HPT was similarly docked to the four PLA_2 homologues. Pronounced negative binding energies were calculated for HPT relative to AFM. The presence of large and electronegative (Cl and S) atoms in the structure of HPT provided more dipole interactions with the amino acid residues. Supplementary Figure 5 depicts the best-docked poses which were oriented such that the said atoms were closer in proximity to polar hydrogen atoms of the amino acid residues. Consequently, the effect of the presence of Ca^{2+} ions from the protein crystal structures was predicted to be less significant for the binding of HPT to PLA_2 homologues relative to that of AFM. Results also demonstrated that the binding energies of HPT to calcium-containing PLA_2 homologues were not favored. The best-docked pose of HPT that gave the highest calculated binding energy, was with HPT to 1S6B, which incidentally was a PLA_2 without Ca^{2+}.

The docking results of HPT were found to be similar to AMB since both exhibited more favorable binding energy values than that of AFM due to the polar regions present. These regions allowed dipole interactions to form with the nearby amino acid residues. Supplementary Figure 6 depicts the optimal docking pose observed with 1PSH (−9.59 kcal/mol) from *Naja naja*, where the Ca^{2+} ion of the protein was in direct contact with one of the oxygen atoms of the docked AMB. A more optimal docking pose was observed for Ca^{2+} free 1S6B (−9.41 kcal/mol) compared to calcium-containing 1LN8 (−8.43 kcal/mol). This was because, in the docking of AMB to 1LN8, the more optimal pose did not allow for the cytoplasmic Ca^{2+} ions to come in contact with the electronegative oxygen atom. The presence of Ca^{2+} ion did not improve the binding energy. In contrast, the best-docked pose of AMB with 1S6B was made possible due to dipole interactions. Although quantum theory allows us to study representative interactions between specific compounds and phospholipase homologues, further experiments such as *in vivo* studies are required to verify the possible mechanism of the anti-venom effect of *A. parvifolia* bark. The thorough evaluation of the anti-venom potential of the extract would require biochemical analysis of the lethality neutralization potential of the preparation in accordance with the recommended WHO protocols for anti-venom production. A comparative study must also be done to evaluate the effectiveness of the extract in relation to commercial anti-venom serum (polyvalent)[36].

In conclusion, *A. parvifolia* demonstrated efficient antioxidant ability and antiproliferative action on mutant immortalized cell lines (MCF-7, H69PR, HT-29, and THP-1) at low IC_{50} values (< 7 μg/mL), which was similar to the positive control zeocin. Moreover, *A. parvifolia* demonstrated non-cytotoxic activity on HDFn cells exhibited by an IC_{50} value greater than 100 μg/mL, whereas HDFn treated with zeocin displayed IC_{50} values less than 5.00 μg/mL. The results of this work indicated that crude (MEOH:DMSO) extracts from *A. parvifolia*, with more in-depth *in vivo* and clinical trials, could be developed into a chemotherapeutic agent or as an adjuvant in the control of human breast adenocarcinoma, human small cell lung carcinoma, human colorectal cancer, and human acute monocytic leukemia. *A. parvifolia* bark also presented remarkable *in vitro* inhibitory activities against $sPLA_2$. *N. philippinensis* venom neutralization through the use of the constituents of *A. parvifolia* bark or in combination therapy with anti-venom serum could be promising inhibitors in the management of snakebite envenoming due to the presence of AFM, HPT, and AMB, which gave exemplary binding energies in the docking results. Findings of this study show *A. parvifolia* bark extract as a potential snake venom inhibitor, however, this can only be further substantiated through *in vivo* experiments as well as neutralization assays.

Conflict of interest statement

The authors declare that there is no conflict of interest.

Acknowledgments

The authors deferentially recognize that the completion of this work was largely due to funding provided by the De La Salle University Science Foundation in coordination with the University Research Coordination Office (Project number: 18 F U 2TAY16-3TAY17). The researchers would similarly like to acknowledge the vital assistance and provision that Professor Michio Murata of the Department of Chemistry, Graduate School of Science, Osaka University, munificently conferred to this endeavor.

Funding

This study is supported by the De La Salle University Science Foundation in coordination with the University Research Coordination Office (Project number: 18 F U 2TAY16-3TAY17).

Authors' contributions

MCST: conceptualization, chemical characterizations, data processing, manuscript writing; MSSC: chemical characterization, data processing, manuscript writing; VCL: collection of plant material, authentication of *Alstonia parvifolia*, manuscript writing; RSM: anti-venom assay, manuscript writing; YIAR: molecular docking simulations, manuscript writing; FCF Jr: molecular docking simulations, manuscript writing; GGO: cytotoxicity assays, data processing, manuscript writing.

References

[1] Madhiri R, Vijayalakshmi G. A review on phytochemical composition and pharmacological aspects of the genus *Alstonia*. *Pharmatutor* 2018; **6**(1): 50-55.

[2] Sarmiento RT. Vegetation of the ultramafic soils of Hinatuan Island, Tagana-An, Surigao Del Norte: An assessment as basis for ecological restoration. *Amb Sci* 2018; **5**(2): 44-50.

[3] Dey A. *Alstonia scholaris* R.Br. (Apocynaceae): Phytochemistry and pharmacology: A concise review. *J App Pharm Sci* 2011; **1**(6): 51-57.

[4] Pratyush K, Misra CS, James J, Lipin DMS, Veettil AKT, Thankamani V. Ethnobotanical and pharmacological study of *Alstonia* (Apocynaceae) – a review. *Int J Pharm Sci Res* 2011; **3**(8): 1394-1403.

[5] Department of Control of Neglected Tropical Diseases. *Snakebite envenoming: A strategy for prevention and control*. Geneva: WHO Document Production Services; 2019, pp. 1-70.

[6] Janardhan B, Shrikanth VM, Mirajkar KK, More SS. *In vitro* screening and evaluation of antivenom phytochemicals from *Azima tetracantha* Lam leaves against *Bungarus caeruleus* and *Vipera russeli*. *J Venom Anim Toxins Incl Trop Dis* 2014; **20**: 12.

[7] Silva A, Isbiser GK. Current research into snake antivenoms, their mechanisms of action and applications. *Biochem Soc Trans* 2020; **48**(2): 537-546.

[8] Ghosh R, Mana K, Sarkhel S. Ameliorating effect of *Alstonia scholaris* L. bark extract on histopathological changes following viper envenomation in animal models. *Toxicol Rep* 2018; **5**: 988-993.

[9] Zhu H, Liu S, Yao L, Wang L, Congfa L. Free and bound phenolics of buckwheat varieties: HPLC characterization, antioxidant activity, and inhibitory potency towards α-glucosidase with molecular docking analysis. *Antioxidants* 2019; **8**(12): 606.

[10]Rahman M, Islam B, Biswas M, Alam AHMK. *In vitro* oxidant and free radical scavenging activity of different parts of *Tabebuia pallida* growing in Bangladesh. *BMC Res Notes* 2015; **8**: 621.

[11]Tan MCS, Carranza MSS, Linis VC, Malabed RS, Oyong GG. Antioxidant, cytotoxicity, and antiophidian potential of *Alstonia macrophylla* bark. *ACS Omega* 2019; **4**(5): 9488-9496.

[12]Trott O, Olson AJ. AutoDock Vina: Improving the speed and accuracy of docking with a new scoring function, efficient optimization, and multithreading. *J Comput Chem* 2009; **31**: 455-461.

[13]Wong KY, Tan CH, Tan NH. Venom and purified toxins of the spectacled cobra (*Naja naja*) from Pakistan: Insights into toxicity and antivenom neutralization. *Am J Trop Med Hyg* 2016; **94**(6): 1392-1399.

[14]Meng Q, Yau LF, Lu JG, Wu ZZ, Zhang BX, Wang JR, et al. Chemical profiling and cytotoxicity assay of bufadienolides in toad venom and toad skin. *J Ethnopharmacol* 2016; **187**: 74-82.

[15]Wu JH, Cao YT, Pan HY, Wang LH. Identification of antitumor constituents in toad venom by spectrum-effect relationship analysis and investigation on its pharmacologic mechanism. *Molecules* 2020; **25**(18): 4269.

[16]Schmeda-Hirschmann G, Quispe C, Arana GV, Theoduloz C, Urra FA, Cardenas C. Antiproliferative activity and chemical composition of the venom from the Amazonian toad *Rhinella marina*. *Toxicon* 2016; **121**(2016): 119-129.

[17]Al-Shanawani AR, Fatani AJ, El-Sayed FH. The effects of a sodium and a calcium channel blocker on lethality of mice injected with the yellow scorpion (*Leiurus quinquestriatus*) venom. *J Venom Anim Toxins Incl Trop Dis* 2005; **11**(2): 175-197.

[18]Batina MF, Cintra AC, Veronese EL, Lavrador MA, Giglio JR, Pereira PS, et al. Inhibition of the lethal and mytotoxic activities of *Crotalus durissus terrificus* venom by *Tabernaemontana catharinensis*: Identification of one of the active components. *Planta Med* 2000; **66**(5): 424-428.

[19]Menecucci CS, Mucellini KL, Oliveira MM, Higashi B, Almeida RTR, Porto C, et al. Latex from *Tabernaemontana catharinensis* (A DC)-Apocynaceae: An alternative for the sustainable production of biologically active compounds. *Ind Crop Prod* 2019; **129**: 74-84.

[20]Puthayanukul P, Laovachirasuwan S, Bavovada R, Pakmanee N, Suttsiri R. Anti-venom potential of butanolic extract of *Eclipta prostrata* against

Malayan pit viper venom. *J Ethnopharmacol* 2004; **90**(2-3): 347-352.

[21]Espmeraldino LE, Souza AM, Sampaio SV. Evaluation of the effect of aqueous extract of *Croton urucurana* Baillon (Euphorbiaceae) on the hemmorrhagic activity induced by the venom of *Bothrops jararaca*, using new techniques to quantify hemorrhagic activity in rat skin. *Pytoey* 2005; **12**(8): 570-576.

[22]Reid IR, Horne A, Mason B, Ames R, Bava U, Gamble GD. Effects of calcium supplementation on body weight and blood pressure in normal older women: A randomized controlled trial. *J Clin Endocrinol Metab* 2005; **90**(7): 3824-3829.

[23]Reid IR, Mason B, Horne A, Ames R, Clearwater J, Bava U, et al. Effects of calcium supplementation on serum lipid concentration in normal older women: A randomized controlled trial. *Am J Med* 2002; **112**(5): 343-347.

[24]Sebastian A, Frassetto LA, Sellmayer DE, Morris Jr. RC. The evolution-informed optimal dietary potassium intake of human beings greatly exceeds current and recommended intakes. *Semin Nephrol* 2006; **26**(6): 447-453.

[25]Pourmorad F, Hosseinimehr SJ, Shahabimajd N. Antioxidant activity, phenol and flavonoid contents of some selected Iranian medicinal plants. *Afr J Biotechnol* 2006; **5**(11): 1142-1145.

[26]Kaur R, Arora S. Alkaloids-important therapeutic secondary metabolites of plant origin. *J Crit Rev* 2015; **2**(3): 1-8.

[27]Hensley K, Robinson KA, Gabbita SP, Salsman S, Floyd RA. Reactive oxygen species, cell signaling, and cell injury. *Free Radic Boil Medic* 2000; **28**(10): 1456-1462.

[28]Gómez-Betancur I, Gogineni V, Salazar-Ospina A, León F. Perspective on the therapeutics of anti-snake venom. *Molecules* 2019; **24**(18): 3276.

[29]Mahringer A, Karamustafa S, Klotz D, Kahl S, Konkimalla VB, Wang Y, et al. Inhibition of *p*-glycoprotein at the blood–brain barrier by phytochemicals derived from traditional Chinese medicine. *Cancer Genomics Proteomics* 2010; **7**(4): 191-205.

[30]Awad AB, Williams H, Fink CS. Effect of phytosterols on cholesterol metabolism and MAP kinase in MDA-MB-231 human breast cancer cells. *J Nutr Biochem* 2003; **14**(2): 111-119.

[31]Bickler PE. Amplification of snake venom toxicity by endogenous signaling pathways. *Toxins* 2020; **12**(2): 68.

[32]Jabeen T, Sharma S, Singh N, Singh RK, Kaur P, Perbandt M, et al. Crystal structure of a calcium-induced dimer of two isoforms of cobra phospholipase A_2 at 1.6 A resolution. *Proteins* 2005; **59**(4): 856-863.

[33]Segelke BW, Nguyen D, Chee R, Xuong NH, Dennis E. Structures of two novel crystal forms of *Naja naja naja* phospholipase A_2 lacking Ca^{2+} reveal trimeric packing. *J Mol Biol* 1998; **279**(1): 223-232.

[34]Fremont DH, Anderson DH, Wilson I, Dennis E, Xuong NH. Crystal structure of phospholipase A_2 from Indian cobra reveals a trimeric association. *Proc Natl Acad Sci U S A* 1993; **90**(1): 342-346.

[35]Gutiérrez J, Lomonte B. Phospholipase A_2 myotoxins from *Bothrops* snake venoms. *Toxicon* 1995; **33**(11): 1405-1424.

[36]Soni P, Bodakhe SH. Antivenom potential of ethanolic extract of *Cordi macleodii* bark against *Naja* venom. *Asian Pac J Trop Biomed* 2014; **4**(Suppl 1): S449-S454.

Antioxidant, cytotoxic, and anti-venom activity of *Alstonia parvifolia* Merr. Bark

Maria Carmen S. **Tan**[1*], Mary Stephanie S. **Carranza**[1], Virgilio C. **Linis**[2], Raymond S. **Malabed**[1,3], Yves Ira A. **Reyes**[1], Francisco C. **Franco**, Jr. [1], Glenn G. **Oyong**[4]

[1]*Chemistry Department, De La Salle University, 2401 Taft Avenue, Manila 1004, Philippines*
[2]*Biology Department, De La Salle University, 2401 Taft Avenue, Manila 1004, Philippines*
[3]*Department of Chemistry, Graduate School of Science, Osaka University, Osaka 563-0034, Japan*
[4]*Molecular Science Unit Laboratory, Center for Natural Sciences and Environmental Research, De la Salle University, 2401 Taft Avenue, Manila 1004, Philippines*

SUPPLEMENTARY DATA

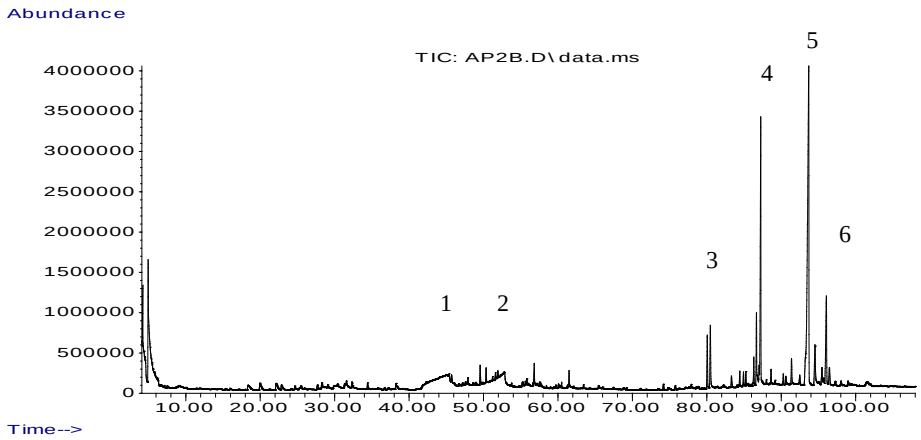

Figure 1. Total ion GCMS chromatogram of MeOH/DMSO extract of *A. parvifolia* bark

Antioxidant, cytotoxic, and anti-venom activity of *Alstonia parvifolia* Merr. Bark

Maria Carmen S. **Tan**[1*], Mary Stephanie S. **Carranza**[1], Virgilio C. **Linis**[2], Raymond S. **Malabed**[1,3], Yves Ira A. **Reyes**[1], Francisco C. **Franco**, Jr. [1], Glenn G. **Oyong**[4]

[1]*Chemistry Department, De La Salle University, 2401 Taft Avenue, Manila 1004, Philippines*
[2]*Biology Department, De La Salle University, 2401 Taft Avenue, Manila 1004, Philippines*
[3]*Department of Chemistry, Graduate School of Science, Osaka University, Osaka 563-0034, Japan*
[4]*Molecular Science Unit Laboratory, Center for Natural Sciences and Environmental Research, De la Salle University, 2401 Taft Avenue, Manila 1004, Philippines*

SUPPLEMENTARY DATA

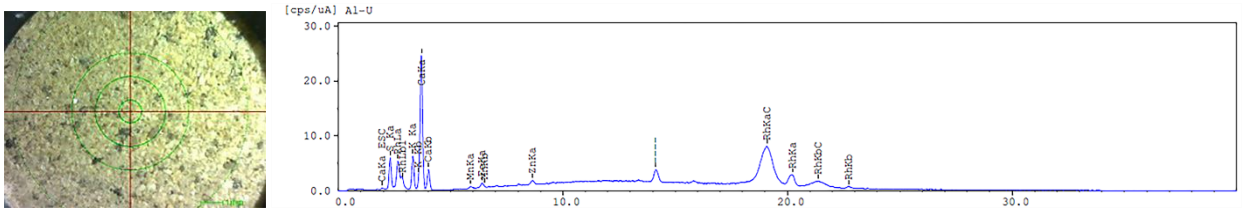

Figure 2. EDX image and X-ray energy spectrum of *A. parvifolia* bark extract.

Antioxidant, cytotoxic, and anti-venom activity of *Alstonia parvifolia* Merr. Bark

Maria Carmen S. **Tan**[1*], Mary Stephanie S. **Carranza**[1], Virgilio C. **Linis**[2], Raymond S. **Malabed**[1,3], Yves Ira A. **Reyes**[1], Francisco C. **Franco**, Jr. [1], Glenn G. **Oyong**[4]

[1]*Chemistry Department, De La Salle University, 2401 Taft Avenue, Manila 1004, Philippines*
[2]*Biology Department, De La Salle University, 2401 Taft Avenue, Manila 1004, Philippines*
[3]*Department of Chemistry, Graduate School of Science, Osaka University, Osaka 563-0034, Japan*
[4]*Molecular Science Unit Laboratory, Center for Natural Sciences and Environmental Research, De la Salle University, 2401 Taft Avenue, Manila 1004, Philippines*

SUPPLEMENTARY DATA

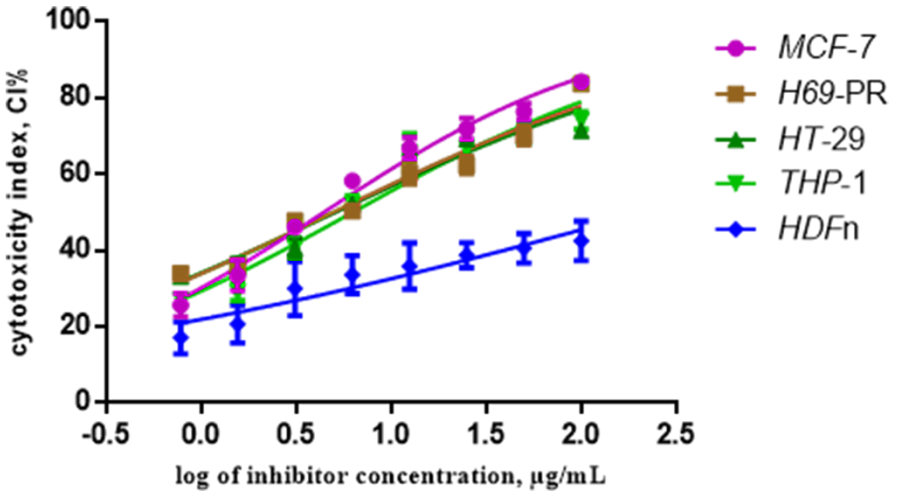

Figure 3. Dose-response curves showing the cytotoxic activities of AP on the cell viability of MCF-7, H69-PR, HT-29, THP-1, and HDFn. Each plot displays the effect of AP against each cell line. Data are shown as mean ± SEM. GraphPad Prism 7.01 was used to perform extra sum-of-squares F-test to (A) evaluate the significance of the best-fit-parameter (half maximal inhibitory concentration) among different treatments, and to (B) determine the differences among the dose-response curve fits. The results are AP, (A) $F(4, 80) = 722.0$, $p < 0.001$ (B) $F(4, 35) = 4.893$, $p = 0.003$.

Antioxidant, cytotoxic, and anti-venom activity of *Alstonia parvifolia* Merr. Bark

Maria Carmen S. **Tan**[1*], Mary Stephanie S. **Carranza**[1], Virgilio C. **Linis**[2], Raymond S. **Malabed**[1,3], Yves Ira A. **Reyes**[1], Francisco C. **Franco**, Jr. [1], Glenn G. **Oyong**[4]

[1]*Chemistry Department, De La Salle University, 2401 Taft Avenue, Manila 1004, Philippines*
[2]*Biology Department, De La Salle University, 2401 Taft Avenue, Manila 1004, Philippines*
[3]*Department of Chemistry, Graduate School of Science, Osaka University, Osaka 563-0034, Japan*
[4]*Molecular Science Unit Laboratory, Center for Natural Sciences and Environmental Research, De la Salle University, 2401 Taft Avenue, Manila 1004, Philippines*

SUPPLEMENTARY DATA

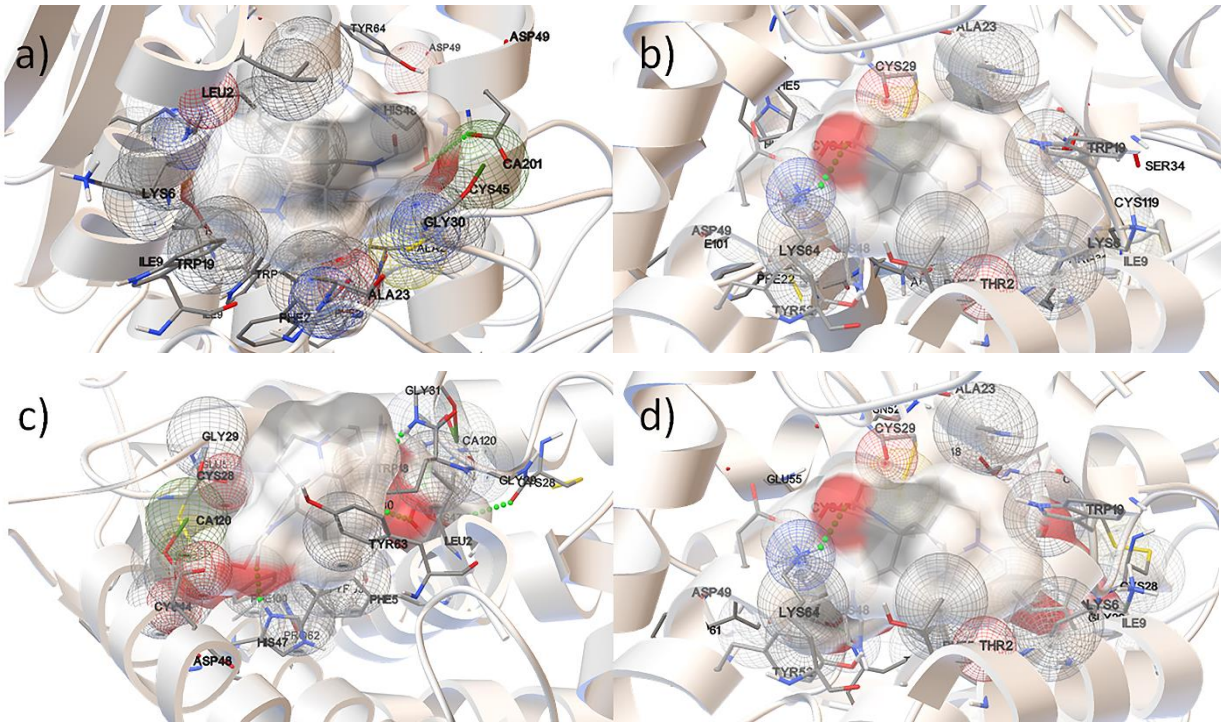

Figure 4. The best docked conformation of AFM, shown in licorice model superimposed with its molecular surface area, in the predicted binding site of each of the candidate target protein: a.) 1LN8, b.) 1S6B, c.) 1PSH, and d.) 1A3F. The protein backbones are depicted by silver ribbon diagrams, while interaction residues are shown in licorice model. Van der Waals interactions are illustrated using wireframe spheres while hydrogen bonds are highlighted with green dotted lines.

Antioxidant, cytotoxic, and anti-venom activity of *Alstonia parvifolia* Merr. Bark

Maria Carmen S. **Tan**[1*], Mary Stephanie S. **Carranza**[1], Virgilio C. **Linis**[2], Raymond S. **Malabed**[1,3], Yves Ira A. **Reyes**[1], Francisco C. **Franco**, Jr. [1], Glenn G. **Oyong**[4]

[1]*Chemistry Department, De La Salle University, 2401 Taft Avenue, Manila 1004, Philippines*
[2]*Biology Department, De La Salle University, 2401 Taft Avenue, Manila 1004, Philippines*
[3]*Department of Chemistry, Graduate School of Science, Osaka University, Osaka 563-0034, Japan*
[4]*Molecular Science Unit Laboratory, Center for Natural Sciences and Environmental Research, De la Salle University, 2401 Taft Avenue, Manila 1004, Philippines*

SUPPLEMENTARY DATA

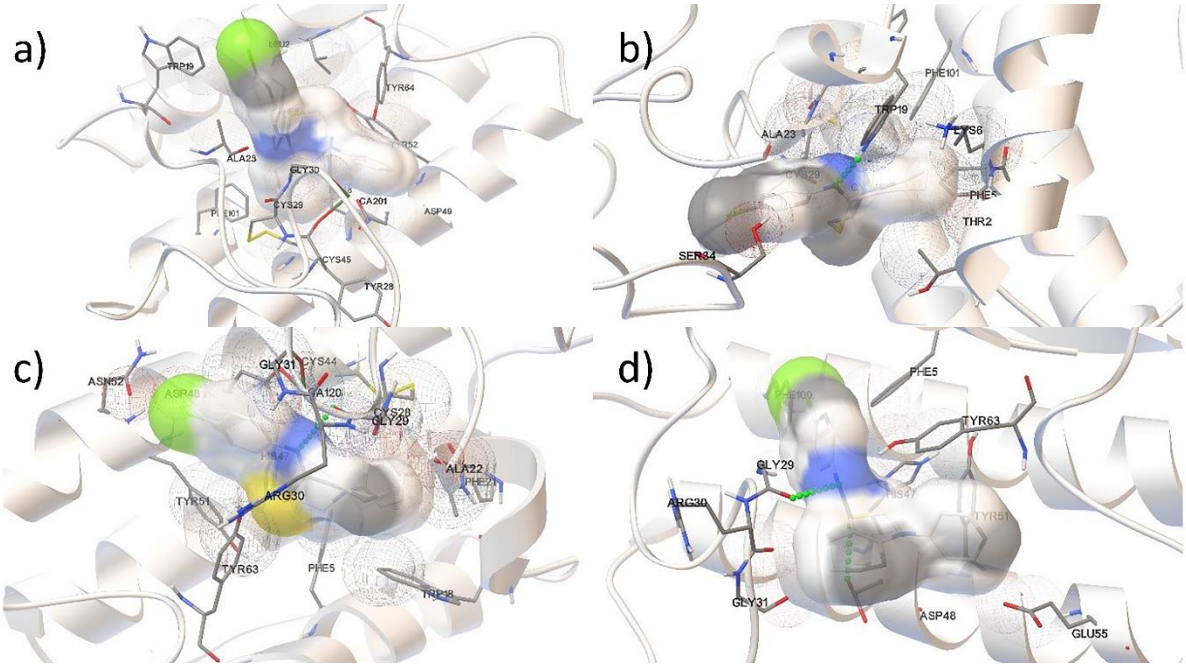

Figure 5. Best docked conformations of HPT shown in licorice model superimposed with its molecular surface area, in the predicted binding site of each of the candidate target proteins: a) ILN8, b) 1S6B, c) 1PSH, and d)1A3F. The protein backbones are depicted by silver ribbon diagrams, while interaction residues are shown in licorice model. Van der Waals interactions are illustrated using wireframe spheres while hydrogen bonds are highlighted with green dotted lines.

Antioxidant, cytotoxic, and anti-venom activity of *Alstonia parvifolia* Merr. Bark

Maria Carmen S. **Tan**[1*], Mary Stephanie S. **Carranza**[1], Virgilio C. **Linis**[2], Raymond S. **Malabed**[1,3], Yves Ira A. **Reyes**[1], Francisco C. **Franco**, Jr. [1], Glenn G. **Oyong**[4]

[1]*Chemistry Department, De La Salle University, 2401 Taft Avenue, Manila 1004, Philippines*
[2]*Biology Department, De La Salle University, 2401 Taft Avenue, Manila 1004, Philippines*
[3]*Department of Chemistry, Graduate School of Science, Osaka University, Osaka 563-0034, Japan*
[4]*Molecular Science Unit Laboratory, Center for Natural Sciences and Environmental Research, De la Salle University, 2401 Taft Avenue, Manila 1004, Philippines*

SUPPLEMENTARY DATA

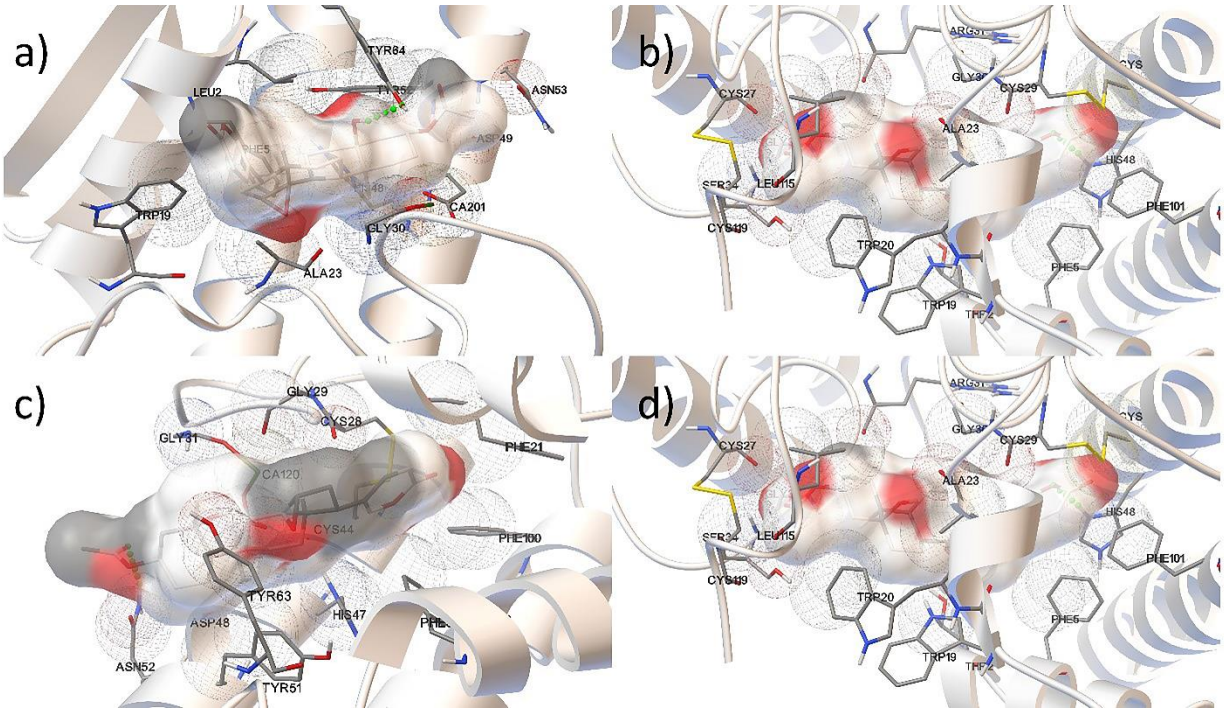

Figure 6. Best docked conformations of AMB shown in licorice model superimposed with its molecular surface area, in the predicted binding site in each of the candidate target proteins: a) ILN8, b) 1S6B, c) 1PSH, and d)1A3F. The protein backbones are depicted by silver ribbon diagrams, while interaction residues are shown in licorice model. Van der Waals interactions are illustrated using wireframe spheres while hydrogen bonds are highlighted with green dotted lines.

Antioxidant, cytotoxic, and anti-venom activity of *Alstonia parvifolia* Merr. Bark

Maria Carmen S. **Tan**[1*], Mary Stephanie S. **Carranza**[1], Virgilio C. **Linis**[2], Raymond S. **Malabed**[1,3], Yves Ira A. **Reyes**[1], Francisco C. **Franco**, Jr. [1], Glenn G. **Oyong**[4]

[1]*Chemistry Department, De La Salle University, 2401 Taft Avenue, Manila 1004, Philippines*
[2]*Biology Department, De La Salle University, 2401 Taft Avenue, Manila 1004, Philippines*
[3]*Department of Chemistry, Graduate School of Science, Osaka University, Osaka 563-0034, Japan*
[4]*Molecular Science Unit Laboratory, Center for Natural Sciences and Environmental Research, De la Salle University, 2401 Taft Avenue, Manila 1004, Philippines*

SUPPLEMENTARY DATA

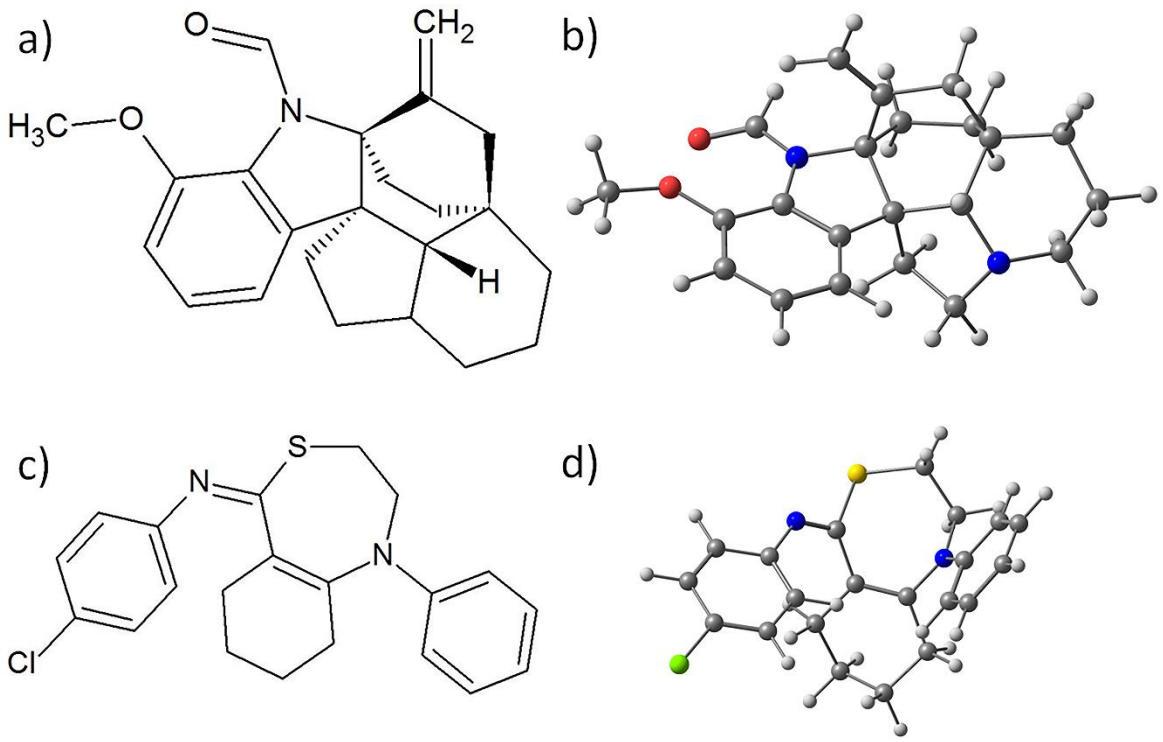

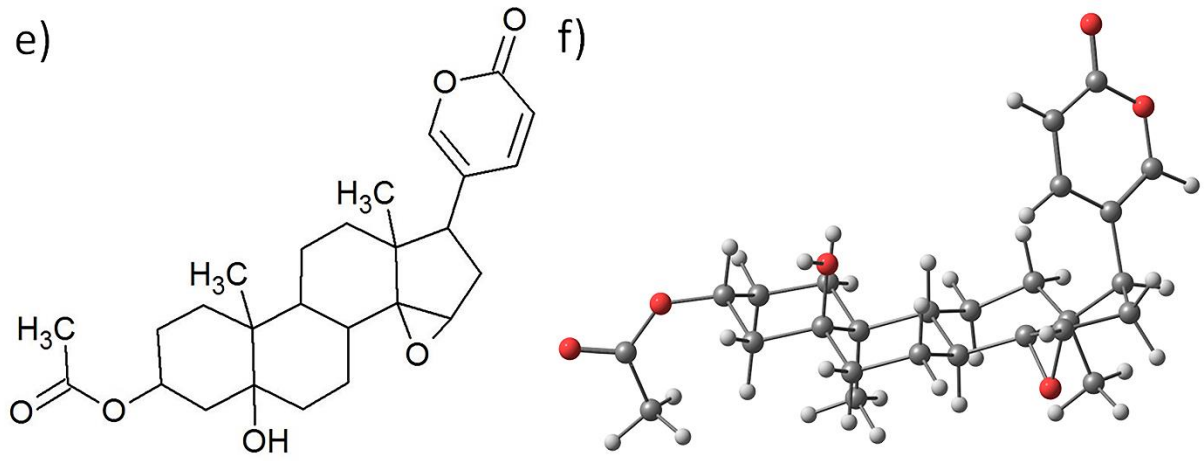

Figure 7. Chemical structures of AFM a) 2D and b) 3D; HPT c) 2D and d) 3D; and AMB e) 2D and f) 3D.

Antioxidant, cytotoxic, and anti-venom activity of *Alstonia parvifolia* Merr. Bark

Maria Carmen S. **Tan**[1*], Mary Stephanie S. **Carranza**[1], Virgilio C. **Linis**[2], Raymond S. **Malabed**[1,3], Yves Ira A. **Reyes**[1], Francisco C. **Franco**, Jr. [1], Glenn G. **Oyong**[4]

[1]*Chemistry Department, De La Salle University, 2401 Taft Avenue, Manila 1004, Philippines*
[2]*Biology Department, De La Salle University, 2401 Taft Avenue, Manila 1004, Philippines*
[3]*Department of Chemistry, Graduate School of Science, Osaka University, Osaka 563-0034, Japan*
[4]*Molecular Science Unit Laboratory, Center for Natural Sciences and Environmental Research, De la Salle University, 2401 Taft Avenue, Manila 1004, Philippines*

SUPPLEMENTARY DATA

Table 1. Top three clusters of AFM conformations docked to candidate targets in *Naja sp*. venom.

Species	PLA_2 homologues	**No. of conformations**	**Highest binding energy (kcal/mol)**
Naja sagittifera	**1LN8**		
	cluster 1	22	-7.89
	cluster 2	36	-6.98
	cluster 3	98	-6.54
	1S6B		
	cluster 1	122	-7.92
	cluster 2	4	-7.10
	cluster 3	21	-7.04
Naja naja	**1PSH**		
	cluster 1	172	-9.68
	cluster 2	2	-8.42
	cluster 3	4	-7.93
	1A3F		
	cluster 1	19	-6.60
	cluster 2	9	-6.51
	cluster 3	170	-6.36

Antioxidant, cytotoxic, and anti-venom activity of *Alstonia parvifolia* Merr. Bark

Maria Carmen S. **Tan**[1*], Mary Stephanie S. **Carranza**[1], Virgilio C. **Linis**[2], Raymond S. **Malabed**[1,3], Yves Ira A. **Reyes**[1], Francisco C. **Franco**, Jr. [1], Glenn G. **Oyong**[4]

[1]*Chemistry Department, De La Salle University, 2401 Taft Avenue, Manila 1004, Philippines*
[2]*Biology Department, De La Salle University, 2401 Taft Avenue, Manila 1004, Philippines*
[3]*Department of Chemistry, Graduate School of Science, Osaka University, Osaka 563-0034, Japan*
[4]*Molecular Science Unit Laboratory, Center for Natural Sciences and Environmental Research, De la Salle University, 2401 Taft Avenue, Manila 1004, Philippines*

SUPPLEMENTARY DATA

Table 2. Top three clusters of HPT conformations docked to candidate targets in *Naja sp*. venom.

Species	PLA_2 homologues	**No. of conformations**	**Highest binding energy (kcal/mol)**
Naja sagittifera	**1LN8**		
	cluster 1	57	-8.74
	cluster 2	105	-7.78
	cluster 3	23	-7.45
	1S6B		
	cluster 1	169	-9.77
	cluster 2	12	-9.53
	cluster 3	9	-8.49
Naja naja	**1PSH**		
	cluster 1	54	-9.66
	cluster 2	34	-9.33
	cluster 3	49	-9.33
	1A3F		
	cluster 1	136	-9.39
	cluster 2	5	-7.83
	cluster 3	10	-7.38

Antioxidant, cytotoxic, and anti-venom activity of *Alstonia parvifolia* Merr. Bark

Maria Carmen S. **Tan**[1*], Mary Stephanie S. **Carranza**[1], Virgilio C. **Linis**[2], Raymond S. **Malabed**[1,3], Yves Ira A. **Reyes**[1], Francisco C. **Franco**, Jr. [1], Glenn G. **Oyong**[4]

[1]*Chemistry Department, De La Salle University, 2401 Taft Avenue, Manila 1004, Philippines*
[2]*Biology Department, De La Salle University, 2401 Taft Avenue, Manila 1004, Philippines*
[3]*Department of Chemistry, Graduate School of Science, Osaka University, Osaka 563-0034, Japan*
[4]*Molecular Science Unit Laboratory, Center for Natural Sciences and Environmental Research, De la Salle University, 2401 Taft Avenue, Manila 1004, Philippines*

SUPPLEMENTARY DATA

Table 3. Top three clusters of AMB conformations docked to candidate targets in Naja sp. venom.

Species	PLA_2 homologues	**No. of conformations**	**Highest binding energy (kcal/mol)**
Naja sagittifera	**1LN8**		
	cluster 1	5	-8.43
	cluster 2	47	-7.66
	cluster 3	11	-7.39
	1S6B		
	cluster 1	41	-9.41
	cluster 2	46	-9.10
	cluster 3	3	-7.62
Naja naja	**1PSH**		
	cluster 1	32	-9.59
	cluster 2	122	-9.41
	cluster 3	38	-9.18
	1A3F		
	cluster 1	128	-7.75
	cluster 2	3	-7.42
	cluster 3	20	-7.22